Research Square

Preprints are preliminary reports that have not undergone peer review.
They should not be considered conclusive, used to inform clinical practice,
or referenced by the media as validated information.

What stands behind luminosity peak of type IIP supernovae?

V. P. Utrobin

utrobin@itep.ru

NRC ``Kurchatov Institute"

N. N. Chugai

Institute of Astronomy, Russian Academy of Sciences

Research Article

Keywords:

Posted Date: November 17th, 2026

DOI: https://doi.org/10.21203/rs.3.rs-11455459/v1

License: This work is licensed under a Creative Commons Attribution 4.0 International License.
Read Full License

Additional Declarations: No competing interests reported.

What stands behind luminosity peak of type IIP supernovae?

V. P. Utrobin[1,2*] and N. N. Chugai[2]

[1*]NRC "Kurchatov Institute", acad. Kurchatov Square 1, Moscow, 123182, Russia.
[2]Institute of Astronomy, Russian Academy of Sciences, Pyatnitskaya St. 48, Moscow, 119017, Russia.

*Corresponding author(s). E-mail(s): utrobin@itep.ru;
Contributing authors: nchugai@inasan.ru;

Abstract

We explore the origin of an initial broad luminosity peak that precedes the light curve plateau in type IIP supernovae. It is well known that the explosion of an evolutionary red supergiant model in the frame of radiation hydrodynamics fails to reproduce the initial luminosity peak. A common practice to compensate this drawback is to introduce massive ($\gtrsim 0.3\,M_\odot$) circumstellar shell attached to the evolutionary model. This remedy, however, has a negative side effect — a strong deceleration of the outer ejecta, which is inconsistent with early spectral data. An alternative way out suggests modification of a hydrogen envelope of the evolutionary red supergiant model — the outer layers should have steeper density gradient. We perform the search for the optimal multi-parameter hydrodynamic model of type IIP SN 1999em based on the Markov Chain Monte Carlo sampling. The major result is that the initial luminous peak is well reproduced by the explosion of the red supergiant with the logarithmic density gradient smaller than -3 in the outer layers of about $0.9\,M_\odot$. We suggest that the mechanism for the density steepening in the hydrogen envelope is closely related to the unknown mechanism responsible for the creation of the ubiquitous low-mass ($<0.01\,M_\odot$) dense confined shell detected in type IIP supernovae.

Keywords: Hydrodynamics – Methods: numerical – Supernovae: general – Supernovae: individual: SN 1999em

1 Introduction

A type IIP supernova (SN IIP) is an explosion of a red supergiant (RSG) that retains a significant part of the hydrogen-rich (hydrogen) envelope until the core collapse. Its light curve is generally understood as the radiative cooling of the expanding fireball that ends up about 100 days with the transition to the radioactive tail — the glow of the cold ejecta powered by the radioactive decay of ^{56}Ni $\rightarrow^{56}$Co $\rightarrow^{56}$Fe. The fireball cooling proceeds through two distinct stages: (i) the initial luminosity peak ($t \lesssim 30$ days) followed by (ii) the luminosity plateau — the gradual cooling in the regime of a cooling recombination wave (CRW) (Grassberg et al., 1971).

With a radiation hydrodynamics code in hand (many of them are open sources) the light curve and the expansion velocities presumably could be easily reproduced by the explosion of an appropriate RSG model. In fact, the outcome of this naive approach would be disappointing. Indeed, the explosion of an evolutionary RSG model in the frame of the one-dimensional (1D) radiation hydrodynamics lacks the Rayleigh-Taylor and turbulent mixing of metals and helium with the hydrogen envelope at the (C+O)/He and He/H

composition interfaces occurring during the explosion. This mixing dramatically affects the light curve (Woosley, 1988). There is no common recipe for the required mixing in the pre-SN. Generally, it is advisable to smooth steep density gradients and mix material of the different composition in a way that is compatible with the late stage of the light curve plateau.

The second failure of the evolutionary RSG model occurs when ones describe the initial luminosity peak (Utrobin and Chugai, 2008). It is proposed that to reproduce the initial peak requires a significantly steeper density gradient in the hydrogen envelope of the RSG model than in the evolutionary one (Utrobin, 2007). The mechanism responsible for steepening the density gradient in the RSG envelope is unknown.

An alternative solution to the luminosity peak problem is to invoke an additional massive ($0.3 - 1\,M_\odot$) circumstellar (CS) shell attached to the evolutionary RSG model (Morozova et al., 2017). The last decade this recipe has gained widespread acceptance. The overlooked drawback of this conjecture is an inevitable deceleration of the outer ejecta that turns out inconsistent with the observational data (cf. Utrobin and Chugai, 2026). This flaw rules out the conjecture of a massive CS shell[1].

The goal of the present communication is to emphasize the point that to solve the problem of the early luminosity peak of SNe IIP one needs to admit that the RSG pre-SN has a steeper density gradient of the hydrogen envelope compared to the evolutionary RSG model. As an example, we consider the well-observed SN 1999em ealier studied hydrodynamically (Baklanov et al., 2005; Utrobin, 2007). The density distribution of the hydrogen envelope will be set by three parameters: the inner and outer gradients with the inflection radius in between. This means that with usual four parameters (the ejecta mass, the explosion energy,the RSG radius, and the extent of ^{56}Ni mixing) we obtain the seven free parameters for the hydrodynamic model.

To cope with the search for the optimal model in the 7D parameter space, we address the Markov Chain Monte Carlo (MCMC) sampling technique. This procedure requires to perform about 7000 – 10 000 samplings for each run. It would take 0.5 yr for the radiation hydrodynamics code CRAB to perform one MCMC run with the available notebook. We therefore use the 300 times faster code VELTEM with the radiation transfer in the equilibrium diffusion approximation.

Since the last time the code VELTEM was used 30 years ago, we briefly reiterate its description (Section 2) with some important numerical aspects never published before. In Section 3.1, we describe our simple approach to fit the hydrodynamic model to the observational data by means of the variation of the principal parameters and apply it to SN 1999em. We then use a more sophisticated approach to get the optimal model with the MCMC technique (Section 3.2). In Section 4 we discuss the obtained results and summarize with the conclusion in Section 5.

Below for SN 1999em, we adopt a distance of 11.7 Mpc (Leonard et al., 2003), a recession velocity of 800 $\mathrm{km\,s^{-1}}$ (Leonard et al., 2002), a total extinction $A_V = 0.31$, and an explosion date of JD 2451476.77 (Baron et al., 2000; Hamuy et al., 2001; Elmhamdi et al., 2003).

2 Hydrodynamic model

The SN hydrodynamic models discussed below are based on a numerical integration of the equations of radiation hydrodynamics in the approximation of equilibrium diffusion limit for a gas that moves with spherical symmetry in its own gravitational field. The integration is performed using our radiation hydrodynamics code VELTEM applied formerly, for example, to SN 1987A (Grassberg et al., 1987; Utrobin, 1993) and SN 1993J (Utrobin, 1994).

The differential equations of radiation hydrodynamics (e.g. Mihalas and Mihalas, 1984), written for Lagrangian coordinates the time t and the mass m enclosed within the sphere of the radius r, are: the velocity definition,

$$\frac{\partial r}{\partial t} = v \,, \tag{1}$$

the continuity equation,

$$\frac{\partial r}{\partial m} = \frac{1}{4\pi r^2 \rho} \,, \tag{2}$$

[1] Surprisingly, numerous papers promoting the massive CS shell never mention the problem of the ejecta deceleration.

the momentum equation,

$$\frac{\partial v}{\partial t} = -4\pi r^2 \frac{\partial (P+Q)}{\partial m} - \frac{Gm}{r^2} \ , \qquad (3)$$

the energy equation,

$$\frac{\partial E}{\partial t} + (P+Q)\frac{\partial}{\partial t}\left(\frac{1}{\rho}\right) = -4\pi \frac{\partial (r^2 F)}{\partial m} + \varepsilon \ . \qquad (4)$$

Here ρ is the gas density, $P = P_g + E_r/3$ is the total pressure of gas and radiation (the radiative internal energy related to the temperature T by $E_r = aT^4$, where a is the radiation constant), $E = E_g + E_r$ is the total specific internal energy of gas and radiation, Q is the artificial viscosity, G is the gravitational constant, F is the radiative flux, and ε is the specific energy deposition rate, for example, due to the radioactive decay of ^{56}Ni. To automatically capture shocks, a simple artificial viscosity (e.g. Richtmyer and Morton, 1967) is added into the hydrodynamic equations.

The diffusion flux of the equilibrium radiation is given by

$$F_D = -4\pi r^2 \frac{c}{3\chi_{\rm R}} \frac{\partial E_r}{\partial m} \ , \qquad (5)$$

where c is the speed of light and $\chi_{\rm R}$ is the Rosseland mean opacity (true absorption and scattering). The radiative flux F, in turn, is represented by the diffusion flux F_D corrected in accordance with a flux-limited diffusion theory of Levermore and Pomraning (1981):

$$F = f(\xi) F_D \ , \qquad (6)$$

where $f(\xi)$ is the flux limiter

$$f(\xi) = \frac{2+3\xi}{2+3\xi+3\xi^2} \ , \ \xi = \frac{|F_D|}{cE_r} \ . \qquad (7)$$

The value cE_r represents the maximum diffusion flux.

As initial conditions for the equations of radiation hydrodynamics we use polytropic-like stellar models in hydrostatic equilibrium. Initial data and boundary conditions are specified to properly formulate this problem: the radius r, the velocity v, and the radiative flux F at the inner boundary and the radiative flux F and a zero gas pressure ($P_g = 0$) at the outer boundary.

The composition is assumed to be a mixture of hydrogen, helium, and an "average" heavy element. At each time step, the ionization equilibrium of this mixture is determined by an approximate method of calculating the multiple ionization of the heavy element. The Rosseland mean opacity is evaluated in the hydrogenic approximation, allowing for Thomson scattering by free electrons.

Especially for this study we add the contribution of spectral lines to the opacity in an expanding medium with a velocity gradient. It is evaluated by the generalized formula of Castor et al. (1975). Oscillator strengths of lines are taken from the line database of Kurucz (2002) containing nearly 530 000 lines. Energy level data are from the atomic spectra database of the National Institute of Standards and Technology. Atomic and ionic level populations are determined by the Boltzmann formulae and the Saha equations for a mixture of all elements from H to Zn with the local temperature.

The transport of γ-rays from the decay chain ^{56}Ni $\rightarrow ^{56}$Co $\rightarrow ^{56}$Fe is treated in an approximation similar to that of Sutherland and Wheeler (1984) with an effective γ-ray absorption opacity of 0.03 cm^2 g^{-1} for an electron to nucleon ratio of 0.5. The latter is inferred by Colgate et al. (1980) from Monte Carlo calculations. Positrons are assumed to deposit their energy locally.

The SN explosion is initiated by a supersonic piston applied to the bottom of the stellar envelope at the boundary of the 1.58 $M_\odot$ central core, which is removed from the computational mass domain and assumed to collapse to become a neutron star.

To handle the system (1-4) described above, we replace the differential equations by suitable discrete approximations and solve these numerically. We divide the medium into discrete cells, locating radii, velocities, and fluxes at cell interfaces and material and radiation properties (density, pressure, energy etc.) at cell centers. We use an implicit form of both the momentum equation (3) and the energy equation (4) to integrate the discretized equations of radiation hydrodynamics.

It is worth noting that in type IIP SNe during the plateau phase the bolometric luminosity is mainly determined by properties of cooling and recombination wave (CRW). This phenomenon was established by Grassberg et al. (1971) and analyzed in detail by Grasberg and Nadezhin

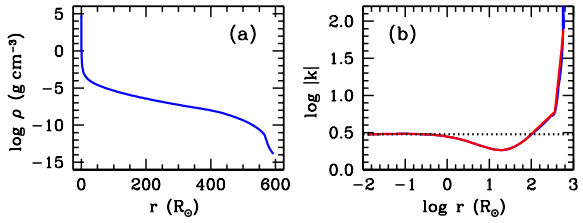


Fig. 1 The pre-SN structure of the VELTEM optimal model. Panel (a): the density distribution as a function of radius. Panel (b): the distribution of the logarithmic density gradient k as a function of radius for the same model (*blue line*). *Red line* is a similar pre-SN model the hydrogen envelope of which is described by following parameters: $R_{base} = 62\,R_\odot$, $R_{ip} = 363\,R_\odot$, $\alpha = 0.52$, and $\beta = 5.35$. *Dotted line* corresponds to the critical value $k = -3$.

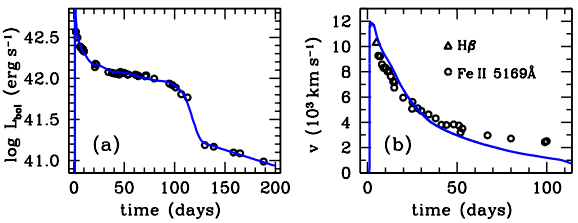


Fig. 2 The bolometric light curve and the evolution of photospheric velocity for the VELTEM optimal model. Panel (a): the model light curve (*blue line*) overlaid on the bolometric data (*circles*) (Elmhamdi et al., 2003). Panel (b): the evolution of model velocity defined by the level $\tau_{\rm Thomson} = 1$ (*blue line*) is compared with the photospheric velocities estimated from the absorption minimum of the Hβ and Fe II 5169 Å lines (Hamuy et al., 2001; Leonard et al., 2002).

(1976). A main property of the CRW consists in generating virtually the entire energy flux carried away by radiation within its front. This radiation flux exhausts the thermal and recombination energy of cooling matter by means of recombination. It was well demonstrated for SN 1999em (Utrobin, 2007). The numerical treatment of the flux in such specific conditions faces difficulties because of the very steep dependence of the opacity on the temperature. The formation of a suitable difference expression for the diffusion flux is presented in Appendix A.

3 Fitting models to data

3.1 Optimal model via parameter variation

A straightforward search for the optimal model is based on the visual estimate of the quality of fitting the observational data. We used this approach in all our previous hydrodynamic studies of various SNe. As to SN 1999em, it was earlier investigated in detail with the Lagrangian radiation hydrodynamics code CRAB (Utrobin, 2007). The inferred basic parameters of the optimal model — the pre-SN radius R_{pSN}, the ejecta mass M_{ej}, the explosion energy E, the ^{56}Ni mass $M_{\rm Ni}$, and its mixing extension M_{mix} — are listed in Table 1. This optimal model is dubbed the CRAB model. It is noteworthy that the RSG pre-SN in this case was nonevolutionary with a steeper density gradient in the hydrogen envelope compared to that of the evolutionary RSG model.

Since here we use a simplified version of the hydrodynamics code VELTEM with the equilibrium-radiation diffusion (Section 2), we produce a reference hydrodynamic model of SN 1999em, the VELTEM model. We construct the pre-SN model (Fig. 1a) similar to that of Utrobin (2007). The optimal model found via the parameter variation describes the bolometric light curve and the expansion velocities (Fig. 2) for the basic parameters listed in Table 1.

To explore the effects of the density distribution of the RSG hydrogen envelope on the bolometric light curve and the expansion velocities, it is desirable to approximate the density profile in a simple way. Fortunately, the plot $\log|k| - \log r$ (Fig. 1b), where $k = d\ln\rho/d\ln r$ is the logarithmic density gradient, reveals the two regions with a power law behavior

$$k(r) = k_0 \left(\frac{r}{r_0}\right)^p , \qquad (8)$$

where r_0 and k_0 are the radius and the value k at the origin of this dependence, respectively, and p is an effective index. In these inner and outer regions, adjacent at the inflection point of the radius R_{ip}, the effective index p is given by

$$p = \begin{cases} \alpha & \text{for } R_{base} < r < R_{ip} , \\ \beta & \text{for } R_{ip} < r < R_{pSN} , \end{cases} \qquad (9)$$

where R_{base} is the radius close to the bottom of the hydrogen envelope.

The above approximation procedure is applied to the density profile of the VERTEM model and results in the following parameter values: $R_{base} = 62\,R_\odot$, $R_{ip} = 363\,R_\odot$, $\alpha = 0.52$, and $\beta = 5.35$. The

Table 1 Comparison of the optimal models for SN 1999em

		CRAB		VELTEM	MCMC	
Parameter	Unit	Value	Error	Value	Value	Error
Pre-SN radius R_{pSN}	$R_\odot$	500	± 200	600	680	$+46\,/-37$
Ejected mass M_{ej}	$M_\odot$	19.0	± 1.2	22.5	21.9	$+0.7\,/-0.7$
Explosion energy E	10^{51} erg	1.3	± 0.1	1.61	1.45	$+0.07\,/-0.07$
^{56}Ni mass $M_{\rm Ni}$	$M_\odot$	0.036	± 0.009	0.036	0.036	–
Extent of ^{56}Ni mixing v_{mix}	km s^{-1}	660	–	1360	1340	$+70\,/-90$
Inflection point R_{ip}	$R_\odot$	–	–	363	378	$+13\,/-13$
Parameter α	–	–	–	0.52	0.52	$+0.02\,/-0.02$
Parameter β	–	–	–	5.35	5.35	$+0.07\,/-0.06$

approximate density distribution (Fig. 1b) agrees well with the original distribution that justifies the use of the accepted approximation.

It is known that the shock decelerates whenever it encounters a density profile that falls off with increasing value ρr^3, while it accelerates for density profiles with decreasing value ρr^3 according to the blast-wave solution (Sedov, 1959). Dotted line in Fig. 1b indicates the critical value $k = -3$ and shows that the velocity of the shock increases when the shock enters the layers with the value $k < -3$ within the region $r > 100\,R_\odot$. This density distribution guarantees a good fit of the hydrodynamic model to the observed light curve and the expansion velocities at the early stage, during the first 30 days (Fig. 2).

3.2 Optimal model via MCMC sampling

A more reliable way to optimize the hydrodynamic model is based on the search of the likelihood maximum via a random walk in multi-parameter space. This technique is realized as the MCMC sampling with the Metropolis-Hastings acceptance function (e.g., Hogg and Foreman-Mackey, 2018).

Our hydrodynamic model for the MCMC study is specified by seven parameters: the pre-SN radius R_{pSN}, the ejecta mass M_{ej}, the explosion energy E, the ^{56}Ni mixing extension M_{mix}, the inflection point radius R_{ip}, the power indices α and β. The first four are the basic parameters in traditional SN hydrodynamic studies, whereas other three describe the structure of the hydrogen envelope — a central point of the present study. The ^{56}Ni mass $M_{\rm Ni}$ is not included to the list, because its value is fixed and well determined by the luminosity at the radiative tail.

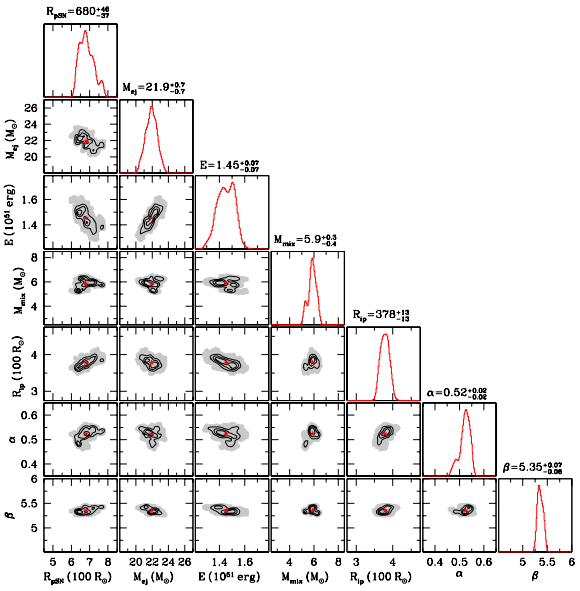


Fig. 3 The posterior constraints on the physical parameters of the optimal hydrodynamic model for the normal type IIP SN 1999em. The contour plots show estimates of the two-dimensional marginalized probability densities and the histograms show the marginalized density for each parameter. The 1σ confidence intervals centered around the median are given at the top of the histograms. *Red stars* mark the positions of these medians in the two-dimensional plots and *gray regions* represent the parameter scatter during the MCMC sampling.

As the observational data set, we use the bolometric light curve, the evolution of the photospheric velocity, and the maximum velocity of the ejecta. The "UBVRI" bolometric light curve of SN 1999em was constructed by Elmhamdi et al. (2003). The photospheric velocities were evaluated from radial velocities at maximum absorption of

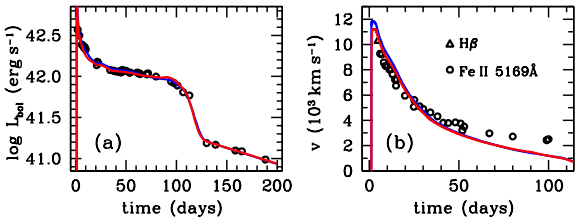


Fig. 4 A comparison of the MCMC optimal model (*red line*) with the VELTEM optimal model (*blue line*). See Fig. 2 legend for details.

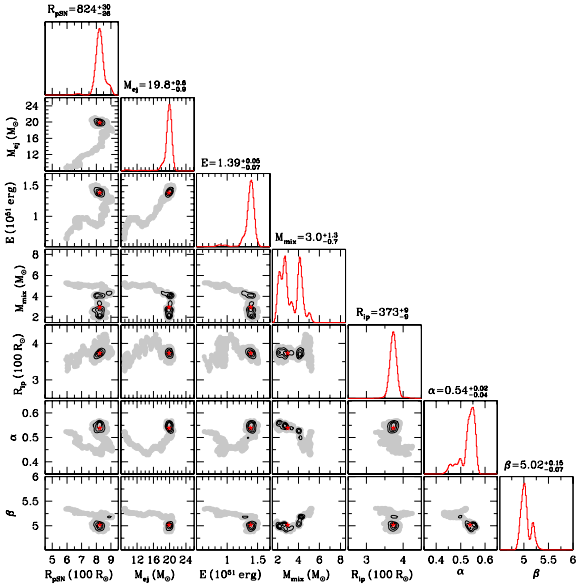


Fig. 5 The travel of the SN hydrodynamic model from a low-mass configuration to the global extreme in the seven parameters space. See Fig. 3 legend for details.

spectral lines Hβ and Fe II 5169 Å measured by Hamuy et al. (2001) and Leonard et al. (2002). In addition, we estimate the maximum velocity of the SN ejecta of $13500 \pm 500\,\mathrm{km\,s^{-1}}$ on JD 2451481.79 from the blue edge of the Hα absorption in the spectrum obtained by Leonard et al. (2002).

The sampling of the parameters is realized as flat priors for all of them. To evaluate the chi-squared (χ^2) function and, consequently, the likelihood function, we compare the calculated hydrodynamic model specified by the sampling with the observables of SN 1999em — the bolometric light curve, the photospheric velocities, and the maximum velocity of the ejecta (Fig. 2).

We start our sampler with the seven parameters of the VELTEM model in Table 1 and then the MCMC code makes 7000 steps. This results in posterior probability distribution functions (pdfs) for these parameters and two-dimensional scatter plots for each parameter pairs shown in the corresponding corner plot (Fig. 3). The medians of these posterior pdfs and the 1σ confidence intervals centered around the medians are given in the corner plot and Table 1. Note that the two-dimensional scatter plots $R_{pSN} - M_{ej}$, $R_{pSN} - E$, and $M_{ej} - E$ show correlation between parameters which is in a agreement with the earlier study (Utrobin, 2007).

The inferred optimal parameters (Table 1) are used as the input data for the hydrodynamic code VELTEM to produce the light curve and the photospheric velocities and then verify them with the observations (Fig. 4). It turns out that the results obtained with the MCMC posterior pdfs are indistinguishable from those achieved by the visual optimization (Fig. 2). This is convincing demonstration that (i) the medians of the posterior pdfs, in fact, represent the MCMC optimal model of SN 1999em and (ii) the visual optimization used previously in all hydrodynamic studies with the code CRAB is a reliable procedure.

Moreover, the optimal model found by the MCMC sampling recovers the density distribution of the hydrogen envelope that is responsible for the description of the initial luminosity peak (Fig. 4). Note that the characteristics of this density profile are very close to those of the VELTEM optimal model (Table 1). This supports the key idea that the steep density gradient of the hydrogen envelope is a mandatory prerequisite for the RSG presupernova of SNe IIP.

Bearing in mind that the outcome of random walk in multi-parameter space might depend on the starting point, it is advisable to check, whether we could miss the solution with a low-mass progenitor. To investigate this problem, we initialize the sampling with the same set of parameters as in the previous MCMC run but a low ejecta mass $M_{ej} = 9\,M_\odot$ and a low explosion energy $E = 0.6 \times 10^{51}$ erg. After 10 000 steps, these two parameters eventually relax at the values of a high ejecta mass and a high explosion energy comparable to those of the MCMC optimal model (Fig. 5). The corner plot demonstrates the absence of hints of a low-mass pre-SN. We conclude, therefore, that the radiation hydrodynamics modeling rules out the pre-SN of SN 1999em significantly less massive

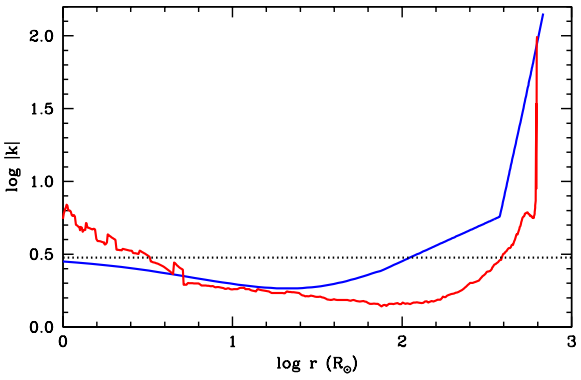


Fig. 6 The distribution of the logarithmic density gradient k as a function of radius for the MCMC pre-SN model (*blue line*). *Red line* is the similar distribution for the evolutionary pre-SN L15 model of Limongi et al. (2000). *Dotted line* corresponds to the critical value $k = d\ln\rho/d\ln r = -3$.

than the earlier estimate of about 21 $M_\odot$ (Utrobin, 2007).

4 Discussion

The optimal model of the well-observed type IIP SN 1999em produced by the MCMC sampling of posterior pdfs for all seven parameters supports the conjecture that the steep density distribution of the RSG hydrogen envelope is responsible for the initial luminosity peak.

The comparison between the density distribution of the hydrogen envelope in the nonevolutionary pre-SN for the MCMC optimal model and that of the evolutionary RSG L15 model (Limongi et al., 2000) is shown in terms of the gradient $k(r)$ (Fig. 6). The plot demonstrates that in the range of $100-600\,R_\odot$ the evolutionary RSG has the gradient $k > -3$ which indicates that the shock wave in this region decelerates, whereas the MCMC optimal model requires $k < -3$ in the same range of radii. The steep density gradient in the outer layers of RSG favors the luminous early light curve via producing the conditions that increase a fraction of the escaped radiation compared to the radiation adiabatic losses in the expanding ejecta. Note that the mass of the external ($r > 100\,R_\odot$) layers with the gradient $k < -3$ in the MCMC pre-SN model is only $0.88\,M_\odot$. Hence, the density distribution of the hydrogen envelope in the evolutionary RSG model should be modified in the outer layers of about $0.9\,M_\odot$ to fit the luminosity peak observed in SNe IIP.

A mechanism for the formation of a steep density gradient of the RSG hydrogen envelope remains to be understood. Yet the spectroscopic data for SN II at the early ($t < 1$ week) stage indicate hydrodynamic processes that take place shortly before the SN explosion. Indeed, there is a strong evidence for an enhanced mass loss during the last years ($\lesssim 10$) before the core collapse. This phenomenon is manifested by the emission lines of hydrogen, helium, and other species with specific "narrow core + broad wings" that originate in the CS dense confined ($r < 10^{15}$ cm) shell (DCS) with the Thomson optical depth of $\sim$3 (Chugai, 2001; Groh, 2014; Yaron et al., 2017). The estimated DCS mass lies in range of $0.003 - 0.007\,M_\odot$ (Yaron et al., 2017; Utrobin and Chugai, 2026) which suggests the tremendous mass-loss rate $\sim 10^{-3}\,M_\odot\,\mathrm{yr}^{-1}$ during $5 - 10$ years before the SN explosion. We suggest that the mechanism responsible for the formation of the low-mass DCS could also produce steepening the density gradient in the outer layers of the RSG hydrogen envelope.

Earlier (Utrobin and Chugai, 2008) we faced a clear disparity between the cumulative distribution of SNe IIP progenitors in the $9 - 25\,M_\odot$ mass range derived from the Salpeter IMF and the distribution of hydrodynamic progenitor masses of SNe IIP. This disparity revealed a pronounced lack of SNe IIP progenitors with the mass lower than $15\,M_\odot$. The growing number of well-observed SNe IIP studied hydrodynamically in a uniform approach does not improve this situation. The current view on this troubling issue was given by Utrobin and Chugai (2025). Given this fundamental problem, of particular interest is the question of an existence of the SN 1999em pre-SN less massive than that of the MCMC optimal model. We answer this question with the special MCMC run confirming that our radiation hydrodynamics studies exclude the pre-SNe of SN 1999em significantly less massive than about $21\,M_\odot$ (Utrobin, 2007).

For many years in our hydrodynamic studies we used the visual optimization and the term "the optimal model" to name our best model, admitting that it is not optimal model in mathematical sense. This study based on the MCMC method convinces us that the visual optimization may be as good as the MCMC sampling, if we take into

account all important observables: the bolometric light curve, the evolution of the photospheric velocity, and the maximum velocity of the ejecta.

5 Conclusion

We have performed the search for the optimal model of the type IIP SN 1999em based on the MCMC sampling posterior pdfs for seven parameters including three parameters describing structure of the RSG hydrogen envelope. The major result is that the initial broad luminous peak is well reproduced by the explosion of the RSG with a steeper density gradient of the hydrogen envelope compared to that of the evolutionary RSG model.

Acknowledgements. The work of V.U. was carried out within the framework of the state assignment of the National Research Center "Kurchatov Institute".

Author contribution. The authors contributed equally to this work.

Funding. Not applicable.

Data availability. No datasets were generated or analyzed during the current study.

Materials availability. Not applicable.

Code availability. Not applicable.

Declarations

Ethics approval and consent to participate

Not applicable.

Consent for publication

Not applicable.

Competing interests

The authors declare no competing interests.

Appendix A

Here we construct an adequate difference expression for the diffusion flux (5), developing the original ideas of Chetverushkin (1985).

To begin with, we represent the difference diffusion flux S at the interface j between the mass cells $\Delta m_{j-1/2}$ and $\Delta m_{j+1/2}$ with the radiative internal energies $U_{j-1/2}$ and $U_{j+1/2}$, respectively, in the following simple form:

$$S_j^{smp} = -\frac{8\pi c}{3} r_j^2 \frac{U_{j+1/2} - U_{j-1/2}}{\Delta m_{j-1/2}\chi_{j-1/2} + \Delta m_{j+1/2}\chi_{j+1/2}} , \tag{A1}$$

which was obtained by Marchuk (1977). We rewrite this expression as

$$S_j^{tau} = -\frac{c}{2\sqrt{3}} \frac{U_{j+1/2} - U_{j-1/2}}{\Delta\tau_{j-1/2} + \Delta\tau_{j+1/2}} , \tag{A2}$$

introducing the optical depths of the corresponding cells

$$\Delta\tau_{j-1/2} = \frac{\sqrt{3}}{16\pi r_j^2} \Delta m_{j-1/2}\chi_{j-1/2} \tag{A3a}$$

$$\Delta\tau_{j+1/2} = \frac{\sqrt{3}}{16\pi r_j^2} \Delta m_{j+1/2}\chi_{j+1/2} . \tag{A3b}$$

As mentioned above, the CRW involves the recombination front which separates the optically thick medium from the thin one. It is clear that at the CRW position the expression (A2) gives unacceptable result when $\Delta\tau_{j-1/2} \to \infty$ and $\Delta\tau_{j+1/2} \to 0$. To overcome this problem, Chetverushkin (1985) solved the radiative diffusion equation at the vicinity of two adjacent cells and obtained the correct difference expression for the diffusion flux. We apply this approach to spherically symmetric geometry and represent a general form of the difference expression which is applicable both at the location of a steep change in the optical depth and outside it.

The radiative diffusion equation (e.g. Zel'dovich and Raizer, 1967) is represented as

$$\frac{dL}{dm} + c\chi(U - U^*) = 0 \tag{A4a}$$

$$16\pi^2 r^4 \frac{c}{3\chi} \frac{dU}{dm} + L = 0 , \tag{A4b}$$

where $L = 4\pi r^2 S$ is the luminosity and $U^* = aT^4$ is the equilibrium radiative internal energy. The difference solution of this equation for the mass interval $[m_j, m_{j+1}]$ with the boundary conditions $U = U_j$ and $L = 4\pi r_j^2 S_j$ at $m = m_j$ and $U = U_{j+1}$

and $L = 4\pi r_{j+1}^2 S_{j+1}$ at $m = m_{j+1}$ is

$$\widetilde{S}_{j+1} - \widetilde{S}_j + c(U_{j+1} + U_j - 2U^*_{j+1/2})A_{j+1/2} = 0 \tag{A5a}$$

$$c(U_{j+1} - U_j) + (\widetilde{S}_j + \widetilde{S}_{j+1})A_{j+1/2} = 0\,, \tag{A5b}$$

where

$$\widetilde{S}_j = \frac{\sqrt{3}}{4\pi r_{j+1/2}^2} L_j\,, \qquad \widetilde{S}_{j+1} = \frac{\sqrt{3}}{4\pi r_{j+1/2}^2} L_{j+1}\,,$$

$$A_{j+1/2} = \tanh\left(\frac{\sqrt{3}}{8\pi r_{j+1/2}^2}\Delta m_{j+1/2}\chi_{j+1/2}\right).$$

Applying the equation (A5b) to the mass intervals $[m_{j-1/2},m_j]$ and $[m_j,m_{j+1/2}]$ and assuming sensibly $L_j = L_{j-1/2} = L_{j+1/2}$ and $r_j = r_{j-1/4} = r_{j+1/4}$, we obtain the correct difference expression for the diffusion flux at the interface j between the optically thick and optically thin cells

$$S_j^{new} = -\frac{c}{2\sqrt{3}}\frac{U_{j+1/2} - U_{j-1/2}}{\tanh\Delta\tau_{j-1/2} + \tanh\Delta\tau_{j+1/2}}\,. \tag{A6}$$

In contrast to the equation (A2), for the equilibrium radiation this expression results in physically sensible limit $S_j^{new} \to (2/\sqrt{3})\sigma T_{j-1/2}^4$ ($\sigma = ac/4$) when $\Delta\tau_{j-1/2} \to \infty$ and $\Delta\tau_{j+1/2} \to 0$.

For the case when both $\Delta\tau_{j-1/2} \to \infty$ and $\Delta\tau_{j+1/2} \to \infty$, however, the obtained expression (A6) is unsatisfactory. To construct a difference expression which is valid both at the location of a steep change in the optical depth and outside it, we define the weight factor

$$q = P(\Delta\tau_{j-1/2})P(\Delta\tau_{j+1/2})\,, \tag{A7}$$

where the auxiliary function

$$P(z) = \frac{\tanh z - z + z^2}{1 - z + z^2} \tag{A8}$$

has the following properties:

$$P(z) \approx \begin{cases} 2z^5/15 & \text{for } z \ll 1\,, \\ 1 - \frac{2\exp(-2z)}{1-z+z^3/3} & \text{for } z > 1\,. \end{cases} \tag{A9}$$

The corresponding properties of the weight factor q permit us to specify the effective optical depth

$$\Delta\tau_j^{eff} = q(\Delta\tau_{j-1/2} + \Delta\tau_{j+1/2}) + (1-q)(\tanh\Delta\tau_{j-1/2} + \tanh\Delta\tau_{j+1/2}) \tag{A10}$$

and, consequently, a general expression of the diffusion flux

$$S_j^{gen} = -\frac{c}{2\sqrt{3}}\frac{U_{j+1/2} - U_{j-1/2}}{\Delta\tau_j^{eff}}\,. \tag{A11}$$

References

Baron, E., Branch, D., Hauschildt, P.H., Filippenko, A.V., Kirshner, R.P., Challis, P.M., Jha, S., Chevalier, R., Fransson, C., Lundqvist, P., Garnavich, P., Leibundgut, B., McCray, R., Michael, E., Panagia, N., Phillips, M.M., Pun, C.S.J., Schmidt, B., Sonneborn, G., Suntzeff, N.B., Wang, L., Wheeler, J.C.: Preliminary Spectral Analysis of the Type II Supernova 1999EM. Astrophys. J. **545**(1), 444–448 (2000) https://doi.org/10.1086/317795 arXiv:astro-ph/0010614 [astro-ph]

Baklanov, P.V., Blinnikov, S.I., Pavlyuk, N.N.: Parameters of the classical type-IIP supernova SN 1999em. Astronomy Letters **31**(7), 429–441 (2005) https://doi.org/10.1134/1.1958107

Castor, J.I., Abbott, D.C., Klein, R.I.: Radiation-driven winds in Of stars. Astrophys. J. **195**, 157–174 (1975) https://doi.org/10.1086/153315

Chetverushkin, B.N.: Mathematical Modelling of Radiative Gas Dynamic Problems (in Russian), (1985)

Chugai, N.N.: Broad emission lines from the opaque electron-scattering environment of SN 1998S. Mon. Not. R. Astron. Soc. **326**(4), 1448–1454 (2001) https://doi.org/10.1111/j.1365-2966.2001.04717.x arXiv:astro-ph/0106234 [astro-ph]

Colgate, S.A., Petschek, A.G., Kriese, J.T.: The luminosity of type I supernovae. Astrophys. J. Lett. **237**, 81–85 (1980) https://doi.org/10.1086/183239

Elmhamdi, A., Danziger, I.J., Chugai, N., Pastorello, A., Turatto, M., Cappellaro, E., Altavilla, G., Benetti, S., Patat, F., Salvo, M.: Photometry and spectroscopy of the Type IIP SN 1999em from outburst to dust formation. Mon. Not. R. Astron. Soc. **338**(4), 939–956 (2003) https://doi.org/10.1046/j.1365-8711.2003.06150.x arXiv:astro-ph/0209623 [astro-ph]

Grassberg, E.K., Imshennik, V.S., Nadyozhin, D.K.: On the Theory of the Light Curves of Supernovae. Astrophys. Space Sci. **10**, 28–51 (1971) https://doi.org/10.1007/BF00654604

Grassberg, E.K., Imshennik, V.S., Nadezhin, D.K., Utrobin, V.P.: Hydrodynamic Models of Supernova 1987A in the Large Magellanic Cloud. Soviet Astronomy Letters **13**, 227 (1987)

Grasberg, E.K., Nadezhin, D.K.: The Cooling Wave in Supernova Shells. Astrophys. Space Sci. **44**(2), 409–428 (1976) https://doi.org/10.1007/BF00642529

Groh, J.H.: Early-time spectra of supernovae and their precursor winds. The luminous blue variable/yellow hypergiant progenitor of SN 2013cu. Astron. Astrophys. **572**, 11 (2014) https://doi.org/10.1051/0004-6361/201424852 arXiv:1408.5397 [astro-ph.HE]

Hogg, D.W., Foreman-Mackey, D.: Data Analysis Recipes: Using Markov Chain Monte Carlo. Astrophys. J. Suppl. Ser. **236**(1), 11 (2018) https://doi.org/10.3847/1538-4365/aab76e arXiv:1710.06068 [astro-ph.IM]

Hamuy, M., Pinto, P.A., Maza, J., Suntzeff, N.B., Phillips, M.M., Eastman, R.G., Smith, R.C., Corbally, C.J., Burstein, D., Li, Y., Ivanov, V., Moro-Martin, A., Strolger, L.G., de Souza, R.E., dos Anjos, S., Green, E.M., Pickering, T.E., González, L., Antezana, R., Wischnjewsky, M., Galaz, G., Roth, M., Persson, S.E., Schommer, R.A.: The Distance to SN 1999em from the Expanding Photosphere Method. Astrophys. J. **558**(2), 615–642 (2001) https://doi.org/10.1086/322450 arXiv:astro-ph/0105006 [astro-ph]

Kurucz, R.L.: Atomic and Molecular Data Needs for Astrophysics. In: Schultz, D.R., Krstic, P.S., Ownby, F. (eds.) Atomic and Molecular Data and Their Applications. American Institute of Physics Conference Series, vol. 636, pp. 134–143 (2002). https://doi.org/10.1063/1.1516330

Leonard, D.C., Filippenko, A.V., Gates, E.L., Li, W., Eastman, R.G., Barth, A.J., Bus, S.J., Chornock, R., Coil, A.L., Frink, S., Grady, C.A., Harris, A.W., Malkan, M.A., Matheson, T., Quirrenbach, A., Treffers, R.R.: The Distance to SN 1999em in NGC 1637 from the Expanding Photosphere Method. Publ. Astron. Soc. Pac. **114**(791), 35–64 (2002) https://doi.org/10.1086/324785 arXiv:astro-ph/0109535 [astro-ph]

Leonard, D.C., Kanbur, S.M., Ngeow, C.C., Tanvir, N.R.: The Cepheid Distance to NGC 1637: A Direct Test of the Expanding Photosphere Method Distance to SN 1999em. Astrophys. J. **594**(1), 247–278 (2003) https://doi.org/10.1086/376831 arXiv:astro-ph/0305259 [astro-ph]

Levermore, C.D., Pomraning, G.C.: A flux-limited diffusion theory. Astrophys. J. **248**, 321–334 (1981) https://doi.org/10.1086/159157

Limongi, M., Straniero, O., Chieffi, A.: Massive Stars in the Range 13-25 M_{solar}: Evolution and Nucleosynthesis. II. The Solar Metallicity Models. Astrophys. J. Suppl. Ser. **129**, 625–664 (2000) https://doi.org/10.1086/313424 astro-ph/0003401

Marchuk, G.I.: Methods of Numerical Mathematics (in Russian), (1977)

Mihalas, D., Mihalas, B.W.: Foundations of Radiation Hydrodynamics, (1984)

Morozova, V., Piro, A.L., Valenti, S.: Unifying Type II Supernova Light Curves with Dense Circumstellar Material. Astrophys. J. **838**(1), 28 (2017) https://doi.org/10.3847/1538-4357/aa6251 arXiv:1610.08054 [astro-ph.HE]

Richtmyer, R.D., Morton, K.W.: Difference Methods for Initial-value Problems, (1967)

Sedov, L.I.: Similarity and Dimensional Methods in Mechanics, (1959)

Sutherland, P.G., Wheeler, J.C.: Models for type I supernovae : partially incinerated white dwarfs. Astrophys. J. **280**, 282–297 (1984) https://doi.org/10.1086/161995

Utrobin, V.P., Chugai, N.N.: Progenitor mass of the type IIP supernova 2005cs. Astron. Astrophys. **491**, 507–513 (2008) https://doi.org/10.1051/0004-6361:200810272 arXiv:0809.3766

Utrobin, V.P., Chugai, N.N.: Type IIP SN 2024bch: hydrodynamic model, shock breakout, and circumstellar interaction. Astrophys. Space Sci. **370**(12), 130 (2025) https://doi.org/10.1007/s10509-025-04522-8 arXiv:2512.01552 [astro-ph.HE]

Utrobin, V.P., Chugai, N.N.: Constraining hydrodynamic model of nearby type IIP SN 2023ixf. Astrophys. Space Sci. **371**(8), 87 (2026) https://doi.org/10.1007/s10509-026-04619-8 arXiv:2606.15395 [astro-ph.HE]

Utrobin, V.: Hydrodynamic study of supernova 1987A: near the peak luminosity. Astron. Astrophys. **270**, 249–258 (1993)

Utrobin, V.: Type IIb supernova 1993J in M 81 : the explosion of a 4 solar mass star in a close binary system. Astron. Astrophys. **281**, 89–92 (1994)

Utrobin, V.P.: An optimal hydrodynamic model for the normal type IIP supernova 1999em. Astron. Astrophys. **461**, 233–251 (2007) https://doi.org/10.1051/0004-6361:20066078 arXiv:astro-ph/0609642

Woosley, S.E.: SN 1987A: After the Peak. Astrophys. J. **330**, 218 (1988) https://doi.org/10.1086/166468

Yaron, O., Perley, D.A., Gal-Yam, A., Groh, J.H., Horesh, A., Ofek, E.O., Kulkarni, S.R., Sollerman, J., Fransson, C., Rubin, A., Szabo, P., Sapir, N., Taddia, F., Cenko, S.B., Valenti, S., Arcavi, I., Howell, D.A., Kasliwal, M.M., Vreeswijk, P.M., Khazov, D., Fox, O.D., Cao, Y., Gnat, O., Kelly, P.L., Nugent, P.E., Filippenko, A.V., Laher, R.R., Wozniak, P.R., Lee, W.H., Rebbapragada, U.D., Maguire, K., Sullivan, M., Soumagnac, M.T.: Confined dense circumstellar material surrounding a regular type II supernova. Nature Physics **13**(5), 510–517 (2017) https://doi.org/10.1038/nphys4025 arXiv:1701.02596 [astro-ph.HE]

Zel'dovich, Y.B., Raizer, Y.P.: Physics of Shock Waves and High-temperature Hydrodynamic Phenomena, (1967)